Chapter 1

The Standard Model

At the basis of all physics at the Large Hadron Collider (LHC) lies the Standard Model. This theory describes all fundamental interactions involving the electroweak and strong forces, as well as the fields which partake in said interactions. In this chapter, we will briefly illustrate the main features of this theory and show how together they paint a complete picture of our current understanding of elementary particle physics.

1.1 An Overview of the Theory

The Standard Model is composed of two sectors: the matter fields and gauge fields. The matter fields are fermionic fields whose excitations lead to the particles which make up ordinary matter, i.e. quarks and leptons. These are intrinsic to the model. The gauge fields, on the other hand, are bosonic fields which arise from symmetries of the model and describe the force-carrying particles, specifically the photon (γ), gluons (g), $W^{\pm}$ and Z^0, as well as the Higgs boson, H^0.

Finish introduction (basic description SM). Then add all sections which may be relevant later on, e.g. continuous and discreet symmetries, parity, V-A, CP violations.

1.2 Gauge Symmetries

1.2.1 QED Lagrangian

We shall now begin to construct the Standard Model Lagrangian. Let us start by considering the free Lagrangian for a massive fermion field, given by the Dirac Lagrangian

$$\mathcal{L}_D = \overline{\psi}(i\partial\!\!\!/ - m)\psi, \tag{1.1}$$

where ψ is the fermion field, $\overline{\psi}$ its Dirac adjoint, and, given the Dirac matrices γ^μ, $\partial\!\!\!/$ is the del operator in Feynman slash notation. It is easy to show that this Lagrangian is invariant under transformations of the type

$$\psi \to \psi' = \exp(ie\alpha)\psi \tag{1.2}$$

where e is a parameter which represents the coupling constant and α is, for now, a parameter independent of the space-time coordinate x. In fact, the analogous transformation for the adjoint field $\overline{\psi}$ is

$$\overline{\psi} \to \overline{\psi'} = [\exp(ie\alpha)\psi]^\dagger\gamma^0 = \psi^\dagger \exp(-ie\alpha)\gamma^0 = \overline{\psi}\exp(-ie\alpha) \tag{1.3}$$

since the operator $\exp(-ie\alpha)$ commutes with γ^0. When applied to the whole Lagrangian, the transformation has the overall effect of leaving the latter unchanged:

$$\mathcal{L}_D \to \mathcal{L}'_D = \overline{\psi'}(i\partial\!\!\!/ - m)\psi' = \overline{\psi}(i\partial\!\!\!/ - m)\psi = \mathcal{L}_D. \tag{1.4}$$

Since the Lagrangian is unchanged, so too are the equations of motion. The transformed fields will therefore have the same dynamics.

We have just shown that the Dirac Lagrangian is invariant under a *global* U(1) gauge symmetry in charge space. At this point, if we want to construct the QED Lagrangian, we must add the kinetic term descrbing the free photon field

$$\mathcal{L}_{kin} = -\frac{1}{4}F^{\mu\nu}F_{\mu\nu} \tag{1.5}$$

where $F_{\mu\nu} = \partial_\mu A_\nu - \partial_\nu A_\mu$, as well as a term describing the interaction between the two fields. We can do this in two ways.

Minimal Coupling

The first, more direct, prescription calls for applying the minimal coupling rule. This requires substituting the four-momentum of the fermion, which we will take to be an electron, with an expression which includes the electromagnetic potential

$$p_\mu \to p_\mu - eA_\mu \tag{1.6}$$

and the coupling constant e. Quantum mechanically, this corresponds to substituting the del operator in the Lagrangian. The Lagrangian thus becomes

$$\mathcal{L}_{QED} = -\frac{1}{4}F^{\mu\nu}F_{\mu\nu} + \overline{\psi}(i\partial\!\!\!/ - eA\!\!\!/ - m)\psi = \mathcal{L}_{kin} + \mathcal{L}_D - e\overline{\psi}\gamma^\mu\psi A_\mu. \tag{1.7}$$

This Lagrangian is still invariant under the same global gauge symmetry as before.

We would like, however, to impose a more stringent symmetry requirement: a *local* gauge symmetry dependent on the space-time coordinate x. Whereas a global symmetry establishes the conservation of a conserved quanity, e.g. electric charge, in any closed system, the local symmetry imposes the same requirement in each point x.

If we promote the gauge symmetry to a local symmetry, i.e. we apply the transformation

$$\psi \to \psi' = \exp[ie\alpha(x)]\psi, \tag{1.8}$$

we find that the Lagrangian is no longer invariant under this transformation due to the action of the derivative. In fact, ignoring the terms which remain invariant, we find that

$$\mathcal{L}' = i\overline{\psi'}\partial\!\!\!/\psi' = i\overline{\psi'}\exp[-ie\alpha(x)]\gamma^\mu\partial_\mu\{\exp[ie\alpha(x)]\psi\} = i\overline{\psi}\partial\!\!\!/\psi - e\overline{\psi}\gamma^\mu\psi\partial_\mu\alpha(x). \tag{1.9}$$

We can use a trick to reobtain the gauge invariance. We know that the electromagnetic tensor $F^{\mu\nu}$ is gauge invariant. This means that if A_μ undergoes the transformation

$$A_\mu \to A'_\mu = A_\mu + \partial_\mu f(x) \tag{1.10}$$

where $f(x)$ is a function such that $\Box f = 0$, then

$$F_{\mu\nu} \to F'_{\mu\nu} = \partial_\mu(A_\nu + \partial_\nu f) - \partial_\nu(A_\mu + \partial_\mu f) = F_{\mu\nu}. \tag{1.11}$$

If we choose f opportunely, we can cancel out the extra term which appears in (1.9) with the last term in (1.7). Specifically, the choice $f(x) = -\alpha(x)$ satisfies our request. Therefore, by combining the transformations (1.8) and (1.10), we can obtain an invariant Lagrangian.

Gauge Principle

The second, more general, way of adding an interaction term to the Lagrangian is by the Gauge Principle. This principle describes a protocol through which we can obtain the dynamics of QED, or any field theory, starting from the global gauge transformation (1.2).

We start, once again, from the Lagrangian (1.1). Having identified the global gauge symmetry of the Lagrangian and having promoted it to a local symmetry, we define the covariant derivative as

$$D_\mu \doteq \partial_\mu + ieA_\mu. \tag{1.12}$$

We then require that the term $D_\mu\psi$ transforms as the field ψ itself

$$D_\mu\psi \to (D_\mu\psi)' = D'_\mu\psi' = \{\partial_\mu + ieA'_\mu\}\psi' = \exp[ie\alpha(x)]D_\mu\psi. \tag{1.13}$$

By developing the equality, we find that A'_μ must be given by

$$A'_\mu = A_\mu - \partial_\mu\alpha(x) \tag{1.14}$$

in order for the Lagrangian to remain invariant.

We can then use the covariant derivative to build a term which describes the free propagation of the field A_μ. We do this by computing the commutator. With some basic algebra, we find that

$$[D_\mu, D_\nu] = ie\{\partial_\mu A_\nu - \partial_\nu A_\mu\} \equiv ieF_{\mu\nu}, \tag{1.15}$$

where $F_{\mu\nu}$ is now a generic tensor of the field A_μ. We thus have

$$F_{\mu\nu} = -\frac{i}{e}[D_\mu, D_\nu]. \tag{1.16}$$

We can then use the field tensor to construct a normalised, gauge invariant Lorentz scalar which will necessarily take the form (1.5). We have thus arrived at the QED Lagrangian in a general way, without assuming any prior knowledge about the field A_μ.

1.2.2 QCD Lagrangian

Armed with the gauge principle, it is now straightforward to derive the QCD Lagrangian. We must note, however, that a few complications arise from the fact that we are now dealing with a non-abelian gauge theory, i.e. a theory whose symmetry group is non-commutative. For a general Yang-Mills theory, the gauge group is $SU(N)$, but in QCD we will be working with $N = 3$.

The Dirac field for the quark can be indicated as q_f^α where f is the flavour index and α is the color index. We know that each flavour comes in three colours, so we can group the fields for each flavour in a three-component vector

$$q_f = \begin{bmatrix} q_f^1 \\ q_f^2 \\ q_f^3 \end{bmatrix}. \tag{1.17}$$

We can thus write the free Lagrangian for the quarks as

$$\mathcal{L}_D = \sum_f \overline{q}_f \left(i\partial\!\!\!/ - m_f\right) q_f \tag{1.18}$$

where m_f is a parameter representing the quark mass and $(i\not{\partial} - m_f)$ is a 3-dimensional diagonal matrix. The quark mass m_f must be understood as a free parameter of the Lagrangian since it is not directly measurable due to the fact that free quarks do not exist in nature.

The Lagrangian is invariant under the following global gauge transformations in colour space:

$$q_f \to (q_f)' = \exp\left[i\theta_a \frac{\lambda^a}{2}\right] q_f \tag{1.19}$$

where θ_a is a parameter and a $= 1, \ldots, 8$ since, in general, the fundamental representation of $SU(N)$ has $N^2 - 1$ generators. λ^a represents the Gell-Mann matrices, which in the fundamental representation of SU(3) can be written as

$$\lambda_1 = \begin{bmatrix} 0 & 1 & 0 \\ 1 & 0 & 0 \\ 0 & 0 & 0 \end{bmatrix}, \quad \lambda_2 = \begin{bmatrix} 0 & -i & 0 \\ i & 0 & 0 \\ 0 & 0 & 0 \end{bmatrix}, \quad \lambda_3 = \begin{bmatrix} 1 & 0 & 0 \\ 0 & -1 & 0 \\ 0 & 0 & 0 \end{bmatrix},$$

$$\lambda_4 = \begin{bmatrix} 0 & 0 & 1 \\ 0 & 0 & 0 \\ 1 & 0 & 0 \end{bmatrix}, \quad \lambda_5 = \begin{bmatrix} 0 & 0 & -i \\ 0 & 0 & 0 \\ i & 0 & 0 \end{bmatrix}, \tag{1.20}$$

$$\lambda_6 = \begin{bmatrix} 0 & 0 & 0 \\ 0 & 0 & 1 \\ 0 & 1 & 0 \end{bmatrix}, \quad \lambda_7 = \begin{bmatrix} 0 & 0 & 0 \\ 0 & 0 & -i \\ 0 & i & 0 \end{bmatrix}, \quad \lambda_8 = \frac{1}{\sqrt{3}} \begin{bmatrix} 1 & 0 & 0 \\ 0 & 1 & 0 \\ 0 & 0 & 2 \end{bmatrix}.$$

The Gell-Mann matrices also allow us to define the structure constant of $SU(3)$, f_{abc}

$$\left[\frac{\lambda_a}{2}, \frac{\lambda_b}{2}\right] = i f_{abc} \frac{\lambda_c}{2}. \tag{1.21}$$

We can now proceed with the gauge principle. We define the covariant derivative as

$$D_\mu = \partial_\mu + i g_s \frac{\lambda_a}{2} G^a_\mu \tag{1.22}$$

where we have introduced the strong coupling constant g_s and 8 spin-1 vector fields G^a_μ. These are the gluon fields. We now promote θ_a to $\theta_a(x)$ and require that $D_\mu q_f$ transform as q_f so as to fix the interaction term between the quarks and the gauge bosons. We find that

$$G^a_\mu \to (G^a_\mu)' = G^a_\mu - \frac{1}{g_s} \partial_\mu \theta^a(x) - f^{abc} \partial_\mu \theta_b(x) G_{\mu c}. \tag{1.23}$$

Last but not least, using the relation

$$-\frac{i}{g_s}[D_\mu, D_\nu] = \frac{\lambda_a}{2} G^a_{\mu\nu} \tag{1.24}$$

we can define the gluon tensor field

$$G^a_{\mu\nu} = \partial_\mu G^a_\nu - \partial_\nu G^a_\mu - g_s f^{abc} G_{\mu b} G_{\nu c} \tag{1.25}$$

which we use to construct the gauge-invariant kinetic term with proper normalisation. We thus find that

$$\mathcal{L}_{QCD} = -\frac{1}{4} G^a_{\mu\nu} G^{\mu\nu}_a + \sum_f \bar{q}_f \left(i\not{D} - m_f\right) q_f. \tag{1.26}$$

1.3 Electroweak Unification

1.3.1 Lagrangian for Pure Weak Interactions

The gauge principle can also be applied to weak interactions. In this case, the fundamental symmetry is $SU_L(2)$, labelled as such because it only applies to left-handed particle states or right-handed anti-particle states. From here on we will consider the particle states, though analagous considerations hold for anti-particle states.

The symmetry acts on a weak-isospin doublet, e.g. (improve notation)

$$\psi_L = \begin{bmatrix} \nu_\ell \\ \ell^- \end{bmatrix}_L \tag{1.27}$$

composed of a left-handed neutrino and a lepton, or in general the left-handed states of any two fermions belonging to the same generation[1]. Corresponding leptonic right-handed states ℓ_R^- are placed in a singlet state, and right-handed neutrino states are not considered as they have not been observed in nature [1].

As before, by applying the local gauge transformations

$$\psi_L \to \psi_L' = \exp\left[i\frac{\tau_j}{2}\alpha^j(x)\right]\psi_L \tag{1.28}$$

$$\ell_R \to \ell_R' = \ell_R \tag{1.29}$$

where i=1,2,3 and τ^i are the generators of $SU(2)$, usually chosen to be the Pauli spin matrices

$$\tau^1 = \begin{bmatrix} 0 & 1 \\ 1 & 0 \end{bmatrix}, \quad \tau_2^2 = \begin{bmatrix} 0 & -i \\ i & 0 \end{bmatrix}, \quad \tau^3 = \begin{bmatrix} 1 & 0 \\ 0 & -1 \end{bmatrix}, \tag{1.30}$$

we can derive the full Lagrangian describing weak interactions

$$\mathcal{L}_W = -\frac{1}{4}W^i_{\mu\nu}W_i^{\mu\nu} + \overline{\psi}_L(i\not{D} - m_i)\psi_L + \ell_R(i\not{\partial} - m_i)\ell_R \tag{1.31}$$

where $D_\mu = \partial_\mu + ig\frac{\tau_j}{2}W^j_\mu(x)$ and g is the weak coupling constant.

The fields $W^1_\mu(x), W^2_\mu(x)$, and $W^3_\mu(x)$ in their raw form are not sufficient to describe the observed phenomenology of weak interactions. By considering

$$W^\pm_\mu = \frac{1}{\sqrt{2}}\left(W^1_\mu \mp iW^2_\mu\right) \tag{1.32}$$

we obtain charged currents which describe the transition from upper and lower components of the weak-isospin doublet observed in nature. Naturally, one would then attempt to identify W^3_μ with the Z^0, however W^3_μ only couples to left-handed particles or right-handed anti-particles, in contrast to what is observed for the physical Z^0.

1.3.2 Electroweak Unification

A more complete description is thus required to match the theory to the physical reality. The Z^0 boson is not the only neutral boson observed in nature: there is also the γ. We can therefore attempt to include electromagnetic interactions in our description of weak interactions and derive the Z^0 and γ fields from two neutral fields.

[1] Quark mixing slightly complicates this.

To this aim, we start by introducing *hypercharge*, defined as

$$Y = 2(Q - I_W^{(3)}) \tag{1.33}$$

This is a quantity meant to replace the $U(1)$ local gauge symmetry of QED, becoming $U_Y(1)$. In this way, we have identified a quantum number capable of distinguishing the states composing the left-handed doublet from the the one composing the right-handed singlet, since, for example the states considered in (1.27) both have hypercharge $Y = -1$ according to this definition, whereas the $SU_L(2)$ singlet state ℓ_R^- has hypercharge $Y = -2$.

We can now consider the full gauge symmetry for electroweak interactions, $SU_L(2) \otimes U_Y(1)$. Under this new gauge symmetry, the transformations (1.28) become

$$\psi_L \to \psi_L' = \exp\left[iy_1\beta(x)\right]\exp\left[i\frac{\tau_j}{2}\alpha^j(x)\right]\psi_L \tag{1.34}$$

$$\ell_R \to \ell_R' = \exp\left[iy_2\beta(x)\right]\ell_R \tag{1.35}$$

where y_1 and y_2 are the hypercharges of the weak isospin doublet and singlet, respectively. The covariant derivatives thus are

$$D_\mu\psi_L(x) = \left[\partial_\mu + ig\frac{\tau_j}{2}W_\mu^j(x) + ig'\frac{y_1}{2}B_\mu(x)\right]\psi_L(x) \tag{1.36}$$

$$D_\mu\ell_R = \left[\partial_\mu ig'\frac{y_2}{2}B_\mu(x)\right]\ell_R(x) \tag{1.37}$$

where g and g' are the two coupling constants, in general different from one another.

We now have four different gauge bosons, $W_\mu^j(x)$ and $B(x)$, which must be identified with the physical gauge bosons $W^\pm$, Z^0 and γ. The physical W bosons can be identified through the relation in (1.32). The mapping from W_μ^3 and B_μ to Z_μ and A_μ can be achieved through a rotation in the neutral sector the gauge bosons

$$\begin{bmatrix} \cos\theta_W & \sin\theta_W \\ -\sin\theta_W & \cos\theta_W \end{bmatrix}\begin{bmatrix} B_\mu \\ W_\mu^3 \end{bmatrix} = \begin{bmatrix} A_\mu \\ Z_\mu \end{bmatrix}. \tag{1.38}$$

If we define the vector

$$\psi = \begin{bmatrix} \nu_{\ell L} \\ \ell_L \\ \ell_R \end{bmatrix} \tag{1.39}$$

and write out the full Lagrangian containing the neutral currents of the electroweak sector of Standard Model,

$$\begin{aligned} \mathcal{L}_{NC} = \overline{\psi}\gamma_\mu &\left\{g\sin\theta_W\frac{\tau_3}{2} + g'\cos\theta_W\frac{Y(\psi)}{2}\right\}\psi A^\mu \\ + \overline{\psi}\gamma_\mu &\left\{g\cos\theta_W\frac{\tau_3}{2} - g'\sin\theta_W\frac{Y(\psi)}{2}\right\}\psi Z^\mu, \end{aligned} \tag{1.40}$$

we can see that we are required to impose a condition on the coefficients in (1.40) to re-obtain the physical currents that we are familiar with. Specifically, the first part of (1.40) corresponds to the interaction term of the Lagrangian (1.7) and the second term corresponds to an interaction term involving a second neutral boson. For the sake of simplicity, we can consider the case of an electron for the purpose of this matching.

The interaction term of (1.7), when specifying the left-handed and right-handed components, corresponds to

$$\mathcal{L} = -e\left[\overline{e}_L\gamma_\mu e_L + \overline{e}_R\gamma_\mu e_R\right]A^\mu. \tag{1.41}$$

fermion	Q	$I_W^{(3)}$	Y_L	Y_R
ν_ℓ	0	$+\frac{1}{2}$	-1	0
ℓ^-	-1	$-\frac{1}{2}$	-1	-2

Table 1.1: Values of parameters

By inspection, we find that

$$-e = g\sin\theta_W \frac{\tau_3}{2} + g'\cos\theta_W \frac{Y(\psi_e)}{2}. \tag{1.42}$$

By specifying τ_3 and $Y(\psi_e)$ to the appropriate component of ψ, in accordance with Table (1.1), we find that

$$g\sin\theta_W = g'\cos\theta_W = e. \tag{1.43}$$

θ_W is the *weak mixing angle*, corresponding to the angle of rotation in neutral sector necessary to achieve the desired mapping. Experimentally, $\sin^2\theta_W$ has been measured to be 0.22290 ± 0.00030, though theoretically it can be parametrized in terms of other quantities as we shall see in the next section.

We can also see that the second neutral current in (1.40) does indeed correspond to the Z current. It is easy to show that the second term of (1.40) can be written as

$$\mathcal{L}_{NC}^{Z} = \overline{\psi}\gamma_\mu \frac{e}{\sin\theta_W\cos\theta_W} Q_Z \psi Z^\mu. \tag{1.44}$$

where $Q_Z = \left\{\frac{\tau_3}{2} - Q\sin^2\theta_W\right\}$. Q_Z is a 3×3 diagonal matrix, allowing for access to each of the components of ψ. It needs to be specified in order to find the full coupling constant. This is straightforward for ν_{eL}: the coupling constant turns out to be $\frac{e}{2\sin\theta_W\cos\theta_W}$.

For the electron, some additional manipulations must first be made since we must deal with the two components. The Lagrangian for the interaction can be written as

$$\mathcal{L}_{NC}^{Ze} = \frac{e}{\sin\theta_W\cos\theta_W}\left\{\overline{e}_L\gamma_\mu Q_Z^L e_L + \overline{e}_R\gamma_\mu Q_Z^R e_R\right\} Z^\mu. \tag{1.45}$$

The projections can be obtained by considering the operators $P_{L/R} = \frac{1}{2}(1\mp\gamma_5)$, i.e.

$$\begin{cases} \overline{e}_L\gamma_\mu e_L = \overline{e}\gamma_\mu \frac{1}{2}(1-\gamma_5)\, e \\ \overline{e}_R\gamma_\mu e_R = \overline{e}\gamma_\mu \frac{1}{2}(1+\gamma_5)\, e. \end{cases} \tag{1.46}$$

The Lagrangian thus becomes

$$\mathcal{L}_{NC}^{Ze} = \frac{e}{\sin\theta_W\cos\theta_W}\left\{\overline{e}\gamma_\mu\frac{1}{2}(Q_Z^L+Q_Z^R)e + \overline{e}\gamma_\mu\frac{1}{2}(Q_Z^L-Q_Z^R)e\right\} Z^\mu. \tag{1.47}$$

$Q_Z^{L/R}$ can be specified directly from (1.44) using the values from Table (1.1). We can use those values to speciy the couplings which appear in (1.47). The Lagrangian simplifies to

$$\mathcal{L}_{NC}^{Ze} = \frac{e}{2\sin\theta_W\cos\theta_W}\overline{e}\gamma_\mu\left\{v_e - a_e\gamma_5\right\} eZ^\mu \tag{1.48}$$

where

$$\begin{cases} v_e = I_W^{(3)}(e_L)\left(1+4Q_e\sin^2\theta_W\right) \\ a_e = I_W^{(3)}(e_L). \end{cases} \tag{1.49}$$

Thus we correctly find that the interaction with the Z can involve both e_L and e_R and that the interaction is of the type V-A, with different coupling constants for the two chiral states of the electron.

The full Lagrangian for electroweak interactions can thus be written as

$$\mathcal{L}_{EW} = \overline{\psi}\left(i\not{D} - m\right)\psi - \frac{1}{4}B_{\mu\nu}B^{\mu\nu} - \frac{1}{4}W^j_{\mu\nu}W^{\mu\nu}_j, \tag{1.50}$$

which, when combined with the rotation in (1.38), gives a correct description of the observed phenomenology.

1.4 Spontaneous Symmetry Breaking

Thus far, we have only considered Lagrangians which contain massless gauge bosons. This is for a very precise reason: mass terms vary under gauge transformations. If we consider, for example, the Proca action for a generic massive bosonic field in an abelian gauge theory

$$\mathcal{L} = -\frac{1}{4}F_{\mu\nu}F^{\mu\nu} - m^2 A_\mu A^\mu \tag{1.51}$$

it is clear that when we apply the transformation (1.10) the Lagrangian is no longer invariant. This is a significant problem since it is known that the $W^\pm$ and Z bosons are massive.

To solve the problem of massive gauge bosons, it is necessary to introduce the *Brout-Englert-Higgs Mechanism* [2, 3], which induces the spontaneous breaking of the gauge symmetry.

This mechanism introduces a scalar field, known as the Higgs field, composed of a weak isospin doublet of two complex scalar fields, or equivalently four real scalar fields

$$\phi(x) = \begin{bmatrix} \phi^+ \\ \phi^0 \end{bmatrix} = \begin{bmatrix} \frac{1}{\sqrt{2}}(\phi_3 + i\phi_4) \\ \frac{1}{\sqrt{2}}(\phi_1 + i\phi_2) \end{bmatrix} \tag{1.52}$$

governed by a complex ϕ^4 theory

$$\mathcal{L} = (\partial_\mu\phi)^\dagger(\partial^\mu\phi) - V(\phi, \phi^\dagger) \tag{1.53}$$

where the potential $V(\phi, \phi^\dagger) = \frac{m^2}{2}\phi^\dagger\phi - \frac{\lambda}{4}(\phi^\dagger\phi)^2$. The components of the doublet, as part of the Electroweak sector of the Standard Model have quantum numbers

$$\begin{cases} I^{(3)}_W(\phi^+) = \frac{1}{2} \\ Y(\phi^+) = 1 \\ I^{(3)}_W(\phi^0) = \frac{1}{2} \\ Y(\phi^0) = 1 \end{cases} \tag{1.54}$$

This means that ϕ^+ carries electrical charge, based on (1.33).

The field ψ_L is added to the Lagrangian (1.50), leading to a Lagrangian which remains invariant under a global $SU_L(2) \otimes U_Y(1)$ gauge symmetry, as is easily verifiable. The symmetry can be promoted to a local gauge symmetry, resulting in the following Langrangian for the Higgs field

$$\mathcal{L} = (D_\mu\phi)^\dagger(D_\mu\phi) - V(\phi, \phi^\dagger) \tag{1.55}$$

where D_μ is the same as in (1.36).

Figure 1.1: The Higgs Potential for an Abelian gauge theory

By minimizing the potential V, we can identify the ground state of the field

$$\frac{\partial V}{\partial |\phi|} = m^2|\phi| + \lambda|\phi|^3 \tag{1.56}$$

If $m^2 > 0$ and $\lambda > 0$, the minimum occurs when $\phi = 0$. However, if we interpret m^2 as a parameter rather than as a mass and allow $m^2 < 0$, we find that there is a local maximum at $\phi = 0$ and a minimum at

$$\langle 0|\, \phi^\dagger \phi\, |0\rangle \equiv (\phi^\dagger \phi)_0 = -\sqrt{\frac{m^2}{\lambda}}. \tag{1.57}$$

The quantum vacuum has thus shifted, as represented in Figure 1.1. The vacuum is *degenerate* since there are infinite values of $\phi^\dagger\phi$ which minimize V. The gauge symmetry is said to be spontaneously broken, in the sense that it is caused solely by the choice of parameters. Since λ is an adimensional quantity, it has the dimensions of energy.

Without loss of generality, we can choose for the vacuum states

$$(\phi_1)_0 = -\sqrt{\frac{m^2}{\lambda}} \equiv \frac{v}{\sqrt{2}},\ (\phi_i)_0 = 0 \tag{1.58}$$

where $i = 2, 3, 4$. Our doublet is thus

$$\phi_0 = \frac{1}{\sqrt{2}} \begin{bmatrix} 0 \\ v \end{bmatrix}. \tag{1.59}$$

The Lagrangian (1.50) along with (1.53) remain invariant under the local gauge transformation, however the vacuum state is no longer invariant under neither the $SU_L(2)$ nor the $U_Y(1)$ local gauge symmetries. For example,

$$\phi_0 \to \phi_0' = \exp\left[ig\frac{\tau_j}{2}\alpha^j(x)\right]\phi \approx \left\{1 + ig\frac{\tau_j}{2}\alpha^j(x) + \ldots\right\}\phi_0 \neq \phi_0 \tag{1.60}$$

Specifically, the invariance is lost due to the action of the generators τ_j. For this reason, these generators are said to be *broken*. Likewise, Y is a broken generator.

Before continuing the discussion, we must first introduce an important theorem involving broken generators.

Theorem 1.4.1 (Goldstone Theorem) *For all continuous global symmetries which do not leave the vacuum state unchanged, there exist corresponding massless particles equal in number to the number of broken generators.*

The theorem holds for global symmetries, however it is also relevant when dealing with local symmetries. In this case, the massless bosons which appear cannot be interpreted as physical particles. They can be gauged away, leading to Higgs-Kibble ghosts which result in *massive* bosons and allow for a physical interpretation of the theory. These ghosts are crucial for our ultimate goal: to give mass to the $W^{\pm}$ and Z while leaving γ massless.

In order to get to our desired result, we must make sure to have one unbroken generator. To obtain it, we can consider the following linear combinations

$$\begin{cases} Q = \frac{\tau_3}{2} - \frac{Y}{2} \\ Q' = \frac{\tau_3}{2} + \frac{Y}{2}. \end{cases} \tag{1.61}$$

It is easy to show that Q is an unbroken generator and Q' is broken. In this way we have obtained 3 broken generators (τ_1, τ_2, Q') and 1 unbroken (Q).

We can now proceed to study the vacuum fluctuations of ϕ. Naively, these can be written as

$$\phi(x) = \frac{1}{\sqrt{2}} \begin{bmatrix} \phi_3(x) + i\phi_4(x) \\ v + \phi_1(x) + i\phi_2(x) \end{bmatrix}, \tag{1.62}$$

though, equivalently, we can write

$$\phi(x) = \frac{1}{\sqrt{2}} \exp\left[\frac{iT_j\xi_j(x)}{2}\right] \begin{bmatrix} 0 \\ v + H(x) \end{bmatrix} \tag{1.63}$$

where T_j are the three $SU(2)$ generators. In the latter form, we have merely parametrized the "naive" expression, as can be seen by expanding the exponential term to first order. The fields $\xi_j(x)$ are the ghosts, which we shall gauge away by choosing the unitary gauge

$$\phi(x) \to \phi'(x) = \exp\left[-\frac{iT_j\xi_j(x)}{2}\right] \phi. \tag{1.64}$$

In accordance with the gauge protocol, this requires a subsequent modification of D_μ, which leads to a modification of the gauge fields, which are said to "eat" the ghosts. After having done so, if we go on to calculate the first term in (1.53) and use (1.32), we find

$$(D_\mu\phi)^\dagger(D_\mu\phi) = \frac{g^2}{4}\left(v^2 + 2vH + H^2\right) W_\mu^+ W^{-\mu} + \frac{1}{8}(v+H)^2 \left(g^2 W_\mu^3 W^{3\mu} - 2gg' W_\mu^3 B^\mu + g'^2 B_\mu B^\mu\right) \tag{1.65}$$

which contains all the physically meaningfull terms. In particular, we can see that (1.65) contains Proca mass terms such as

$$\frac{g^2}{4} v^2 W_\mu^+ W^{-\mu} \equiv M_W^2 W_\mu^+ W^{-\mu}. \tag{1.66}$$

We can then follow the same logic as in that used to derive the unified Electroweak theory and map B_μ and W_μ^3 to A^μ and Z_μ, respectively. After doing so, the second term in (1.65) becomes

$$\frac{1}{8}(g^2 + g'^2)(v+H)^2 Z_\mu Z^\mu \tag{1.67}$$

and we can see that there is no mass term for A_μ, no interaction term involving the Higgs field $H(x)$ and A_μ and that the Z acquires the mass $M_Z^2 = \frac{v^2}{4}(g^2 + g'^2)$. We can also see that the coupling of the Higgs boson to the other bosons is proportional to those bosons' mass.

We have succeeded in giving mass to the three weak gauge bosons. The choice of parameters λ and m^2 spontaneously breaks the gauge symmetry, and the interaction of the field ϕ with the potential generates would-be Goldstone bosons which manifest as ghosts. The choice of unitary gauge allows for the gauge bosons to eat the ghosts, thus gaining mass. The energy scale at which the gauge symmetry is spontaneously broken, known as the vacuum expectation value, is given by v, which in numerical terms corresponds to 246 GeV. Above this energy, the electromagnetic force and the weak nuclear force become one unified electroweak force.

1.5 Yukawa Lagrangian

A similar problem occurs when considering the mass terms for fermions. In this case, the mass term appearing in the Dirac Lagrangian (1.1) does not respect the $SU_L(2) \otimes U_Y(1)$ gauge symmetry due to the fact that the left and right-handed components of the spinor transform differently

$$-m\overline{\psi}\psi = -m\left(\overline{\psi}_R\psi_L + \overline{\psi}_L\psi_R\right). \tag{1.68}$$

This problem can be solved by introducing an interaction with the Higgs field. An infinitesimal $SU(2)$ local gauge transformation has the following effect on the Higgs

$$\phi \to \phi' = \left\{1 + ig\frac{\tau_j}{2}\alpha^j(x)\right\}\phi. \tag{1.69}$$

On the other hand, the same transformation has the opposite effect on $\overline{\psi}_L$

$$\overline{\psi}_L \to \overline{\psi}'_L = \overline{\psi}_L\left\{1 - ig\frac{\tau_j}{2}\alpha^j(x)\right\}. \tag{1.70}$$

Therefore, if we consider the combination $\overline{\psi}_L\phi$, we find that this is a gauge invariant quantity. The same holds true for the $U(1)$ gauge symmetry. Since ℓ_R transforms independently from ψ_L, we can add it to the combination so as to account for the right-handed component as well. Thus the Lagrangian

$$\mathcal{L}_Y = -k\left(\overline{\psi}_L\phi\ell_R + \overline{\ell}_R\overline{\phi}\psi_L\right) \tag{1.71}$$

where k is a coupling constant, is invariant under a $SU_L(2) \otimes U_Y(1)$ local gauge transformation. We can take once again the electron as an example and specify the terms in (1.71). We find that

$$\mathcal{L}_Y = -\frac{kev}{\sqrt{2}}\left(\overline{e}_Le_R + \overline{e}_Re_L\right) - \frac{keH}{\sqrt{2}}\left(\overline{e}_Le_R + \overline{e}_Re_L\right). \tag{1.72}$$

We thus find the Dirac mass term

$$m_e = \frac{kev}{\sqrt{2}} \tag{1.73}$$

as well as a term which couples the Higgs to the fermion field. This term is proportional to the fermion's mass.

In contrast to the derivation of the gauge bosons' mass, the derivation of the fermionic masses is ad-hoc. The fermionic mass terms depends on the coupling k which must be measured from experiment. There is no explanation for the observed mass hierarchy of the fermions.

Discuss Quark mixing? Neutrino mixing?

1.6 The Standard Model Lagrangian

We are now ready to put all the ingredients discussed together and bake the cake that is the Standard Model. The full Lagrangian for the model is given by

$$\mathcal{L}_{SM} = \mathcal{L}_{QCD} + \mathcal{L}_{EW} + \mathcal{L}_{SSB} + \mathcal{L}_{Y}. \tag{1.74}$$

$\mathcal{L}_{QCD}$ describes all strong interactions, $\mathcal{L}_{EW}$ describes electroweak interactions, $\mathcal{L}_{SSB}$ gives mass to the gauge bosons and $\mathcal{L}_{Y}$ gives mass to the fermions. There are a few additional complications due to quark mixing and neutrino mixing which for the sake of brevity we shall pass over.

$\mathcal{L}_{SM}$ is invariant under the full $SU_C(3) \otimes SU_L(2) \otimes U_Y(1)$ local gauge symmetry. In this form, the Lagrangian is purely classical: it must then be quantized and renormalized [4] in order to fully describe our quantum world.

Chapter 2

Collisions at the LHC

One of the best ways to explore the Standard Model is through high-energy particle collisions. The LHC is a 27 km hadron-hadron circular collider where two protons or nucleons interact with each other in a multitude of ways, resulting in a myriad of possible final states. By identifying these final states, and selecting those which correspond to processes of interest, it is possible to study these processes in detail. A number of detectors, including ATLAS and CMS, lie on the beam pipe for this purpose.

The LHC has undergone several phases. During Run 1, the LHC ran at a center of mass energy $\sqrt{s}$ of 7-8 TeV. The energy was increased to $\sqrt{s} = 13$ TeV during Run 2. Run 2 delivered a total integrated luminosity of 156 fb^{-1}. During Run 3, set to begin next year, the $\sqrt{s}$ could increase up to 14 TeV, and it is expected that the integrated luminosity will double to 300 fb^{-1}. In this chapter, we will describe the physics of hadron colliders.

2.1 Factorization

The proton is a dyamic system. In a simplistic view, it is composed of three valence quarks, u, u, d but these are bound together by gluons. The gluons interact both with the valence quarks and themselves, leading to a "sea" composed of gluons as well as quarks and anti-quarks of all flavors. This sea is dominant at low energies, and suppressed at higher energies.

When two hadrons collide at high energies, the resulting interaction does not directly involve the hadrons as a whole but the *partons* which constitute the hadron. Relativistic considerations allow us to deduce that the time-scale is such that only interactions with one parton per hardon are possible. Indeed, in the rest frame of the proton, the time-scale of the interactions holding the proton together are of the order $1/m_p$. In the laboratory frame of the collision, this is boosted by a factor $\gamma = \sqrt{s}/2m_p$. Since the energies available at the LHC place us firmly in the ultrarelativistic limit, interactions with a virtual particle of energy $Q^2 \gg m_p^2$ occur on a time-scale much shorter than γ/m_p, the parton probed has no time to communicate with the other partons.

After the constituent parton has been struck, the virtual particles emitted by the constituent as part of normal interactions within the hadron can no longer be reabsorbed. This effect is exacerbated at higher Q. The end result is a perturbative evolution of the final state particles from the interaction, together with these liberated virtual particles, down to energies of the order of the Landau pole of QCD, Λ_{QCD}. At these energies, due to the running of the coupling constant α_S it is no longer possible to describe QCD using perturbative physics. What follows is the hadronization process, where final state particles undergo non-perturbative interactions

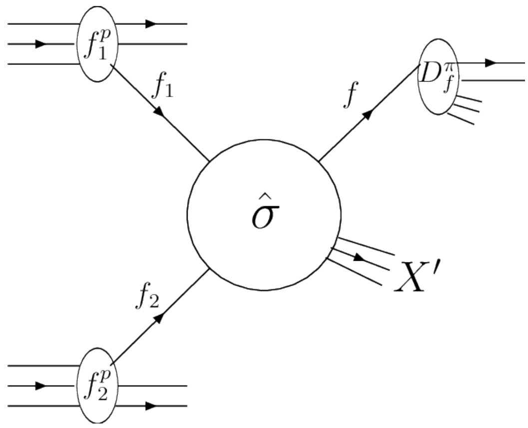

Figure 2.1: A schematic representation of factorization in a process which results in the production of pion in a proton-proton collision [9].

which transform them into relatively long-lived hadrons. Since the time-scale for hadronization is much longer when compared to the elementary process, the cross section for the collision is said to be *factorized* into a hard process descrbied by an elementary cross section and functions describing the non-perturbative physics involved in the hadron before the interaction as well as the hadronization process.

This discussion can be neatly summarized in a formula:

$$\frac{d\sigma}{dX} = \sum_{j,k} \int dx_1 dx_2\ f_j(x_1, Q^2) f_k(x_2, Q^2)\ \frac{d\hat{\sigma}_{jk}(x_1 P_1, x_2 P_2, Q^2, \mu_F^2)}{d\hat{X}}\ F(\hat{X} \to X; Q^2, \mu_F^2). \quad (2.1)$$

Here, we are stating that the differential cross section with respect to a hadronic observable X can be written in terms of the parton-level cross section $d\hat{\sigma}/d\hat{X}$, differential in the parton-level observable $\hat{X}$. $f_j(x_1 P_1, \mu_F)$ and $f_k(x_2 P_2, Q^2)$ are known as Parton Distribution Functions (PDFs) and describe the probability of extracting a parton of type j or k with momentum fraction x_1 or x_2, respectively from the colliding hadrons with momenta P_1 and P_2 when probed at energy Q^2. We must sum over all possibile partons, and integrate over all momentum fractions. Finally, the function $F(\hat{X} \to X; Q^2, \mu_F^2)$ is known as the Fragmentation Function (FF), and describes the non-perturbative transition from partonic states to hadronic states. We will describe the involved functions in more detail in subsequent sections. Figure 2.1 is a schematic representation of factorization in a proton-proton collision.

2.2 Parton Distribution Functions

As previously mentioned, Parton Distribution Functions contain information regarding the constituents of a hadron. To better understand them, we shall study in detail the process known as Deep Inelastic Scattering (DIS).

2.2.1 Deep Inelastic Scattering

DIS is a process which probes the insides of hadrons using leptonic probes. In this section we will focus on high-energy electron-proton inelastic scattering. In this process, the incoming electron

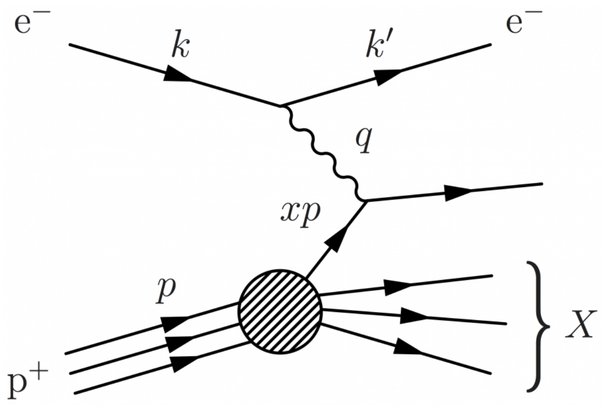

Figure 2.2: A schematic representaiton of the DIS process.

exchanges a virtual photon (if below the production threshold of the massive gauge bosons) with the proton. Specifically, we will look at the proccess

$$e^- \; p \rightarrow e^- \; X \tag{2.2}$$

where X represents an undetermined hadronic final state, mediated by a virtual photon.

Kinematics

A number of kinematic variables are needed to fully describe the process. Without loss of generality, we will work in the targert rest frame (TRF), where the struck proton is at rest. With reference to Figure 2.2, we have

$$\begin{cases} k^\mu = (E, 0, 0, E) \\ p^\mu = (m_p, 0, 0, 0) \\ k^{\mu\prime} = (E', E' \sin\theta, 0, E' \cos\theta) \\ q^\mu = k^\mu - k^{\mu\prime} \end{cases} \tag{2.3}$$

where k^μ and $k^{\mu\prime}$ refer to the four-momenta of the initial and final state electron, respectively, p^μ the four-momentum of the initial state proton and q^μ to the four momentum of the virtual photon. The quantities E and E' refer to the respective energies of the electron in the initial and final state, and θ is the angle at which the electron is scattered with respect to its initial momentum $\vec{k}$.

The first kinematic variable to consider is the energy of the virtual probe, known also as the scale of the process. Since DIS is a space-like process, the four-momentum of the virtual probe $q^2 < 0$, therefore we take

$$Q^2 = -q^2. \tag{2.4}$$

Next we introduce a series of Lorentz-invariant variables. The first variable, y, is defined as

$$y = \frac{p \cdot q}{p \cdot k} \overset{\text{TRF}}{=} 1 - \frac{E'}{E}. \tag{2.5}$$

As is clear, in the TRF, y represents the fraction of energy lost during the inelastic process. For this reason, $0 \leq y \leq 1$. Next, we introduce a similar variable

$$\nu = \frac{p \cdot q}{m_p} \overset{\text{TRF}}{=} E - E' \tag{2.6}$$

which in the TRF represents the the energy lost by the electron in the scattering process. Finally, we introduce the variable Bjorken x, defined as

$$x = \frac{Q^2}{2p \cdot q} \stackrel{\text{TRF}}{=} \frac{Q^2}{2m_p \nu} \tag{2.7}$$

If we consider the definition of the invariant mass of the system,

$$W^2 = (p+q)^2 = p^2 + 2p \cdot q + q^2 = m_p^2 + Q^2 \left(\frac{1}{x} - 1 \right) \geq m_p^2 \tag{2.8}$$

it becomes clear that x represents the “elasticity” of the process: x is limited to the range $0 \leq x \leq 1$, and $x = 1$ corresponds to a perfectly elastic collsion, whereas $x = 0$ corresponds to a perfectly inelastic one. By definition, the Deep Inelastic limit of this process is the limit in which $Q^2 \to \infty$ while x is held constant.

Cross Section

It is possible to calculate the cross section for the inelastic scattering process described above. The most general Lorentz-invariant cross section for the interaction considered is

$$\frac{d^2\sigma}{dxdQ^2} = \frac{4\pi\alpha^2}{Q^4} \left[\left(1 - y - \frac{m_p^2 y^2}{Q^2} \right) \frac{F^2(x,Q^2)}{x} + y^2 F_1(x,Q^2) \right]. \tag{2.9}$$

In the deep inelastic limit, this simplifies to

$$\frac{d^2\sigma}{dxdQ^2} \approx \frac{4\pi\alpha^2}{Q^4} \left[(1-y) \frac{F^2(x,Q^2)}{x} + y^2 F_1(x,Q^2) \right]. \tag{2.10}$$

F_1 and F_2 are *structure functions*, which describe the internal structure of the proton. This cross section corresponds to the hadronic cross section of equation (2.1). It is a crucial ingredient in determining PDFs.

Bjorken Scaling and the Callan-Gross Relation

An important observation involving the aforementioned structure functions is *Bjorken scaling*. This is the observation that, to first order, F_1 and F_2 are independent of Q^2, as shown in Figure 2.3. In addition to this scaling, experimental observations also found that, at sufficiently large Q^2

$$F_2(x) = 2xF_1(x). \tag{2.11}$$

This relation is known as the Callan-Gross relation and is shown in Figure 2.4. We would expect to see scaling if the scattering occured against point-like particles, giving evidence to the composite nature of the proton. In addition to this, the Callan-Gross relation tells us that the constituent partons carry spin-1/2. We therefore have experimental evidence to support the statement that the proton is composed of point-like spin-1/2 particles, namely quarks [1]. The incoming electron elastically scatters against these constituents, explaining these observations and justifying the formula (2.1).

If we consider the DIS process in the infinite momentum frame, defined as the frame in which the energy of the proton in the initial state $E_p \gg m_p$, i.e. $p^\mu = (E_p, 0, 0, E_p)$, we can deduce that the four-momentum of the struck quark can be written as

$$p_q^\mu = (\xi E_p, 0, 0, \xi E_p) \tag{2.12}$$

[1] The proton also has a significant gluon component, as will be discussed in a later section

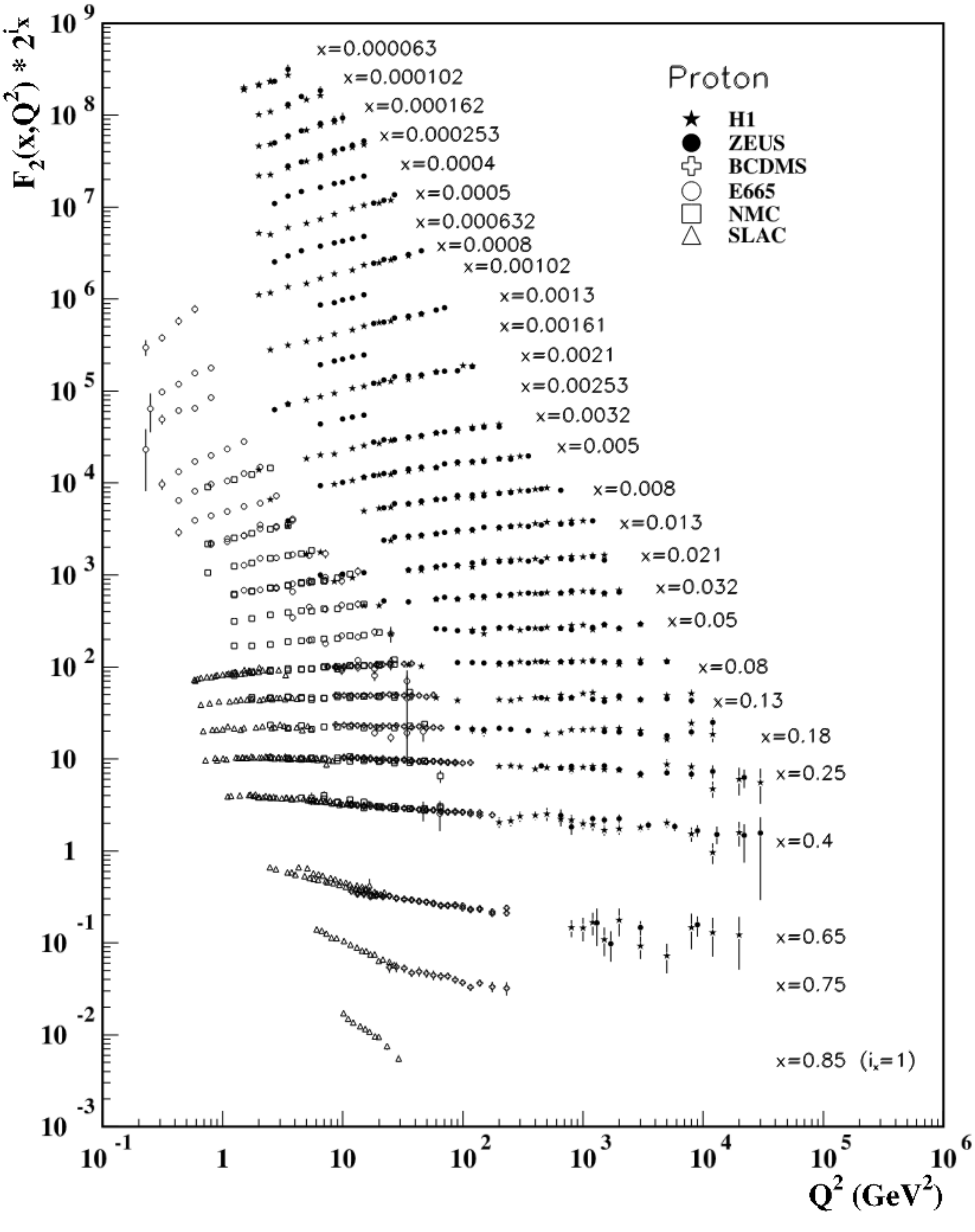

Figure 2.3: The observation of approximate scaling at various experiments. The observed violations are caused by higher-order contributions [10].

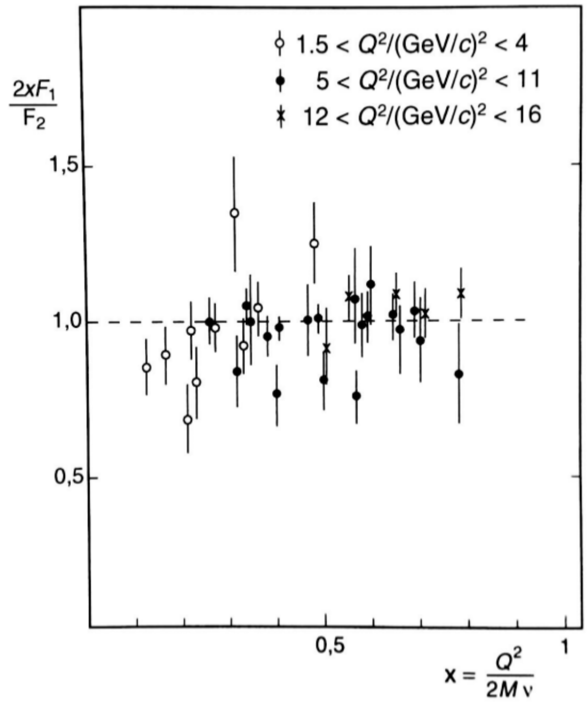

Figure 2.4: An experimental observation of the Callan-Gross relation - Needs citation

where ξ represents the fraction of the proton's momentum carried by the quark. The quark in the final state of the electron-quark scattering will have four-momentum

$$(\xi p + q)^2 = \xi^2 p^2 + 2\xi p \cdot q + q^2 = m_q^2. \tag{2.13}$$

For this relation to hold, we must have $2\xi p \cdot q + q^2 = 0$, which implies that

$$\xi = \frac{-q^2}{2p \cdot q} = \frac{Q^2}{2p \cdot q} = x. \tag{2.14}$$

We can therefore identify x Bjorken with the momentum fraction of the struck constituent quark.

Determining PDFs

We can now proceed in actually determining the constituents of the proton. Experimentally, this is done using formula (2.1), which in the case of DIS becomes

$$\frac{d\sigma}{dE'd\Omega} = \sum_f \int_0^1 dx \, \frac{d\hat{\sigma}}{dE'd\Omega}(xP, q) \, \phi_f(x). \tag{2.15}$$

Should integrate cross section in dE'? The partonic cross section is easily calculable in QED

$$\frac{d\hat{\sigma}}{dE'd\Omega} = \frac{4\alpha^2}{Q^4} E'^2 \cos^2 \frac{\theta}{2} e_f^2 \frac{2m_f x}{Q^2} \delta\left(x' - x\right) \left[1 + \frac{Q^2}{2m_f^2} \tan^2 \frac{\theta}{2}\right]. \tag{2.16}$$

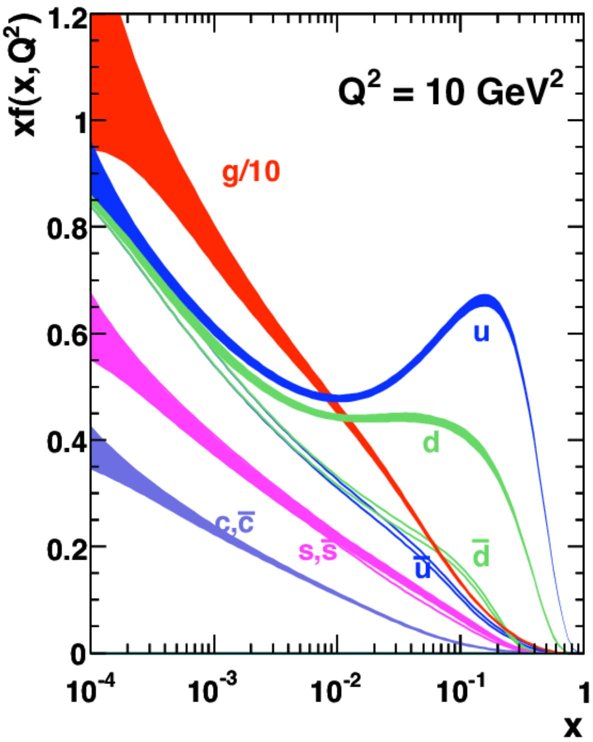

Figure 2.5: PDFs of the proton measured at various values of x at $Q^2 = 10$ GeV^2 [11].

By inserting (2.10) and (2.16) in (2.15), we find that

$$\begin{cases} F_1(x) = \frac{1}{2}\sum_f e_f^2 \phi_f(x) \\ F_2(x) = x\sum_f e_f^2 \phi_f(x). \end{cases} \tag{2.17}$$

We have managed to describe the structure functions in terms of the PDFs, and in turn found the Callan-Gross relation!

By experimentally measuring the cross-section (2.15), we can deconvolve the PDF contribution. Figure 2.5 shows the PDFs of various partons within the proton, measured by ... at $Q^2 = 10$ GeV^2.

PDFs have the notable property of being *universal*. This means that, regardless of what is used to probe them, they will always be the same since they are an intrinsic property of a given hadron. Given this property, determining the proton PDFs is fundamental for making accurate predictions at the LHC.

Gluon PDF

The discussion up to now has focused exclusively on quarks, since, within the original framework of the so-called *Quark Parton Model*, did not include gluons. However, Figure 2.5 shows that, particularly at small x, a significant fraction of the proton's constituents are gluons.

The gluon PDF can be determined in a manner analogous to the quark PDFs. With DIS, we must, however, consider higher-order QCD corrections to be able to study elementary processes such as $\gamma g \to q\bar{q}$. This is not ideal since the process of interest is suppressed. Alternatively, we can look at hadron-hadron collisions, where gluon interactions do appear at leading order.

PDF Evolution

In general, PDFs are functions both of the momentum fraction x and the scale of the hard process Q^2. To first order, this dependence is negligible, but the inclusion of the gluon leads to higher-order QCD corrections which lead to the scaling violations observed.

PDFs cannot be calculated from first principles; they must be measured from experiment. Thankfully, it is not necessary to perform measurements at different values of x and Q^2 to fully determine PDFs.

The Dokshitzer-Gribov-Lipatov-Altarelli-Parisi (DGLAP) Equations allow us to calculate the evolution of a PDF from the scale Q^2 to a different scale Q'^2. This is a notable achievement, as the PDFs can be measured at a certain energy, but re-utilized in a theoretical prediction for a process occuring at a different energy scale.

For the sake of brevity, we shall limit ourselves to citing this incredible result, rather than deriving the whole equation, sennò davvero qui non ne usciamo più.

The evolution equation for the parton density is:

$$\frac{dq_f(x,Q^2)}{d\log Q^2} = \frac{\alpha_s}{2\pi}\int_x^1 \frac{dy}{y}\left[q_f(y,Q^2)P_{qq}\left(\frac{x}{y}\right) + g(y,Q^2)P_{gq}\left(\frac{x}{y}\right)\right]. \tag{2.18}$$

This equation states that, to calculate the PDF for a parton of flavor f at a given x and Q^2 we need only to integrate the parton and gluon PDFs at y and Q^2, along with the splitting functions P_{qq} and P_{qg}. P_{qq} gives the probability of finding a real quark q with momentum fraction x/y after the emission of a virtual gluon, and P_{gq} which is the analogous function for the emission of a real gluon and virtual quark after the splitting

$$\begin{cases} P_{qq}(z) = C_F \frac{1+z^2}{(1-z)_+} \\ P_{qg}(z) = T_R\left[z^2 + (1-z)^2\right] \end{cases} \tag{2.19}$$

where $C_F = (N_c^2 - 1)/2N_c$ is the Casimir invariant of $SU(3)$, T_R is the trace of the Gell-Mann matrices and the plus-prescription has been used to regularize the divergent integral.

An analogous function exists for the evolution of the gluon PDF

$$\frac{dg(x,Q^2)}{d\log Q^2} = \frac{\alpha_s}{2\pi}\int_x^1 \frac{dy}{y}\left[\sum_f q_f(y,Q^2)P_{gq}\left(\frac{x}{y}\right) + g(y,Q^2)P_{gg}\left(\frac{x}{y}\right)\right] \tag{2.20}$$

where this time

$$\begin{cases} P_{gq}(z) = C_F\left[\frac{1+(1-z)^2}{z}\right] \\ P_{gg}(z) = 2C_A\left[\frac{1-z}{z} + \frac{z}{(1-z)_+} + z(1-z)\right] \end{cases} \tag{2.21}$$

where C_A is the Casimir operator for the adjoint representation of $SU(3)$.

2.3 Fragmentation Functions

Fragmentation functions play a role similar to that of PDFs, but rather than describing the possibile initial states of the interaction, they describe the possibile final states that may be observed.

To understand the FFs, it is the *semi-inclusive* DIS process, where we observe one hadron in the final state. The kimatic variables are the same as in (2.3), though we must now include the four-momentum of the final-state hadron

$$P_h^\mu = (E_h, \vec{P_h}) \tag{2.22}$$

and one additional Lorentz invariant variable

$$z_h = \frac{P \cdot P_h}{P \cdot q} \overset{\text{TRF}}{=} \frac{E_h}{\nu} \tag{2.23}$$

which in the TRF represents the fraction of energy lost in the hadronization process of the observed particle.

The cross section can again be calculated without difficulty:

$$\frac{d\sigma}{dxdydz} = \frac{4\pi\alpha_S^2}{Q^4}\left(\frac{y}{2} + 1 - y\right) x \sum_f e_f^2 \phi_f(x) D_f(z) \tag{2.24}$$

where the sum over all flavors includes the anti-quarks. In this way, the FF $D_f(z)$ represents the probability of finding a hadron with fraction ¡ of the available energy. The cross section remains factorized, allowing for information on the FFs by comparison with data, as neither they are calculable in QCD. Finally, it should be said that the FFs depend on the quark from which they originate, hence the index.

2.4 Jets

Due to the non-perturbative nature of the hadronization process and the myriad of particles produced, it is not possible to calculate cross-sections for all of the different possibile hadronic final states. Instead, *jets* are considered in their place. Jets are, as the name suggests, groups of collimated particles. They can be treated as singular objects, allowing for a notable simplification of the calculations.

2.4.1 Jet Definitions

In order to be able to precisely calculate jet cross-sections and confront these with experimental data, it is necessarily to unambiguosly *define* what a jet is. There are multiple possible definitions of jets, and we will briefly some examples of these.

Cone Algorithms

Historically, cone algorithms were the first class of jet algorithms introduced. The very first algorithm was used to classify jets in e^+e^- collisions and depended on two arbitrary parameters, δ and ϵ. If an event had a fraction of energy of at least $1 - \epsilon$ concentrated within two cones of half-angle δ, then that even was said to contain two jets [12]. The fact that the definition relied on arbitrary parameters meant that these had to be specified so that the predictions could be compared to data. This remains a general feature of jet algorithms to this day.

Cone algorithms have progressed in the years since their inception. Today, two of the most widely used code algorithms are iterative and fixed cone algorithms. In iterative cone algorithms, the direction of the jet is initially set by a particle i. All particles within distance R_{ij}

$$\Delta_{ij}^2 = (y_i - y_j)^2 + (\phi_i - \phi_j)^2 < R_{ij} \tag{2.25}$$

in the rapidity/azimuthal angle plane are then taken as part of the jet, and their momenta are summed. The result of this summation is then used as the new seed, and the process is iterated until the jet cone is stable. To fully specify the algorithm, one must choose how to take the seed, and what to do when jets overlap.

Fixed cone algorithms function similarly. In this case, rather than iterating the cone direction, a cone is fixed around a seed, and that cone is called a jet. The particles within the radius R_{ij} are assigned to the jet, and removed from the event record. The algorithm proceeds until all possible jets have been identified.

kt-Algorithms

kt algorithms are part of a family of algorithms known as sequential recombination jet algorithms. The kt algorithms use a momentum-weighted distance

$$\begin{cases} d_{ij} = min(k_{ti}^{2p}, k_{tj}^{2p})\frac{\Delta_{ij}^2}{R^2} \\ d_{iB} = k_{ti}^{2p} \end{cases} \tag{2.26}$$

to establish which particles j lie closest to the particle i. If d_{ij} is less than the distance between i and the beam d_{iB}, i and j are combined into a jet. This procedure iterates over all particles.

These definitions also depend on two parameters: p and R. There exist three noteworthy cases: $p = 1$ is known as the kt algorithm, and weights the distance d_{ij} using the square of the transverse momentum of the softer particle; $p = 0$ is known as the Cabridge-Aachen algorith, and features no weighting; $p = -1$ is known as the anti-kt algorithm, and weights the distance using the inverse of the square of the transverse momentum of the harder particle.

Due to the distance used, the anti-kt algorithm tends to cluster soft particles together with hard particles. This is a useful property as it tends to lead to jets centered about hard particles, and correctly recombines the soft radiation emitted from the hard seed together with that seed. If the hard particles are well-separated, this also leads to conical jets, as shown in Figure 2.6.

2.4.2 Jet Cross Sections

Once we have defined our jets, we can go on to calculate jet cross sections. Without going into too much detail, we will just illustrate a general feature which highlights the usefulness of jets.

If we calculate the two-hadron semi-inclusive cross section for e^+e^- into hadrons, we find that

$$\frac{d\sigma}{dydz_1dz_2} = N_c\frac{\pi\alpha^2}{Q^2}(1+\cos\theta)\sum_f e_f^2 D_f(z_1)D_f(z_2), \tag{2.27}$$

where again the sum over the flavors f runs over both quarks and antiquarks. N_c stands for the number of colors that can be produced, and θ is the angle between the momentum of the quarks produced and the momentum of the colliding leptons, assuming a collinear collision.

If rather than observing the two final-state hadrons we observe the jets surrounding them, the Fragmentation Functions reduce to δ-functions. After integrating over z_1 and z_2, as it is no longer meaningful to consider these quantities, we find that

$$\frac{d\sigma^{jets}}{dy} = N_c\frac{\pi\alpha^2}{Q^2}(1+\cos\theta)\sum_f e_f^2. \tag{2.28}$$

This is exactly the QED cross secction for e^+e^- annihilation! The use of jets allows us to notably simplify calculations while still allowing for accurate predictions, since we neither have to consider fully inclusive cross sections, nor a fully exclusive one.

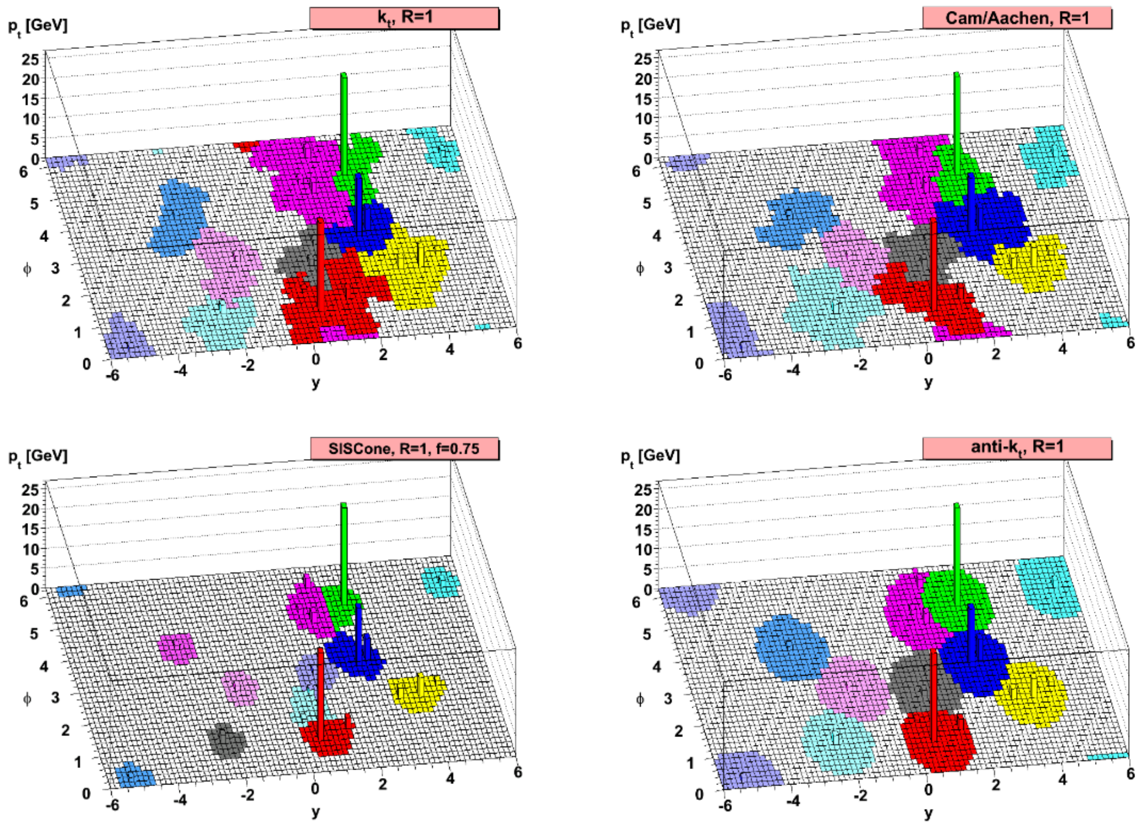

Figure 2.6: A representation of the jets formed from the same event using the three main kt algorithms as well as SISCone, a commonly used cone algorithm. The jets clustered using anti-kt are conical, and centered around the hard particles [13].

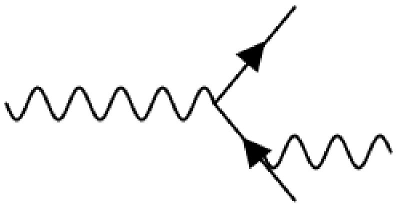

Figure 2.7: A Feynman diagram depicting a real emission in QED.

2.5 Higher Order Corrections

A number of higher order corrections to the elementary cross section are possible. These include real and virtual corrections in all possibile combinations. In QCD, we currently know how to treat corrections up to $\mathcal{O}(\alpha_S^3)$ for a few select processes citation. In this section we will breifly discuss the importance of higher order corrections, as well as some challenges which arise during their calculation.

2.5.1 Infrared and Collinear Divergences

The matrix element for a radiative correction in QED and QCD is easily calculable using the Feynman rules. For example, for the diagram shown in Figure 2.7, the matrix element for all possible real emissions and all possible photon polarizations is found to be

$$\frac{d\sigma}{d\Omega} = \left(\frac{d\sigma}{d\Omega}\right)_0 \frac{\alpha}{2\pi}\left[2\frac{p_- \cdot p_+}{p_- \cdot k p_+ \cdot k} - \frac{m_e^2}{(p_- \cdot k)^2} - \frac{m_e^2}{(p_+ \cdot k)^2}\right]\frac{d^3k}{\omega} \tag{2.29}$$

where $\left(\frac{d\sigma}{d\Omega}\right)_0$ represents the tree-level cross section. In the center-of-mass frame, where the kinematic variables can be expressed as

$$\begin{cases} p_-^\mu = (E, 0, 0, \beta E) \\ p_+^\mu = (E, 0, 0, -\beta E) \\ k^\mu = (\omega, \omega \sin\theta\cos\phi, \omega\sin\theta\sin\phi, \omega\cos\theta) \end{cases} \tag{2.30}$$

where $\beta = \sqrt{1 - \frac{m_e^2}{E^2}}$, (2.29) becomes

$$\frac{d\sigma}{d\Omega} = \left(\frac{d\sigma}{d\Omega}\right)_0 \frac{\alpha}{2\pi}\frac{1}{\omega}\frac{\beta^2\sin^2\theta}{(1-\beta^2\cos^2\theta)^2} d\omega\, d\cos\theta \tag{2.31}$$

where we have already integrated in $d\phi$ This expression is divergent in two cases: when the radiated particle is either very soft ($E \ll 1$) or when it is collinear to the lepton from which it is emitted ($\theta \ll 1$). These cases are known as *infrared* and *collinear* divergences, respectively, and they are problematic as they prohibit the calculation of the cross section at next-to-leading order.

Integrating in $d\cos\theta$ resolves the collinear divergence

$$\frac{d\sigma}{d\Omega} = \left(\frac{d\sigma}{d\Omega}\right)_0 \frac{1}{\omega}\frac{2\alpha}{\pi}\left[\frac{\beta^2+1}{2\beta}\ln\left(\frac{1+\beta}{1-\beta}\right) + 1\right] d\omega \tag{2.32}$$

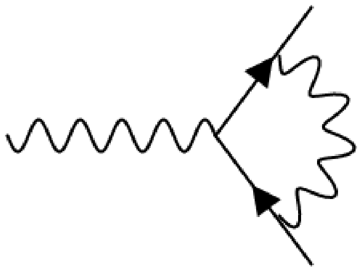

Figure 2.8: A Feynman diagram depicting a virtual correction in QED.

which, when we consider that $s \gg m^2$ simplifies to

$$\frac{d\sigma}{d\Omega} = \left(\frac{d\sigma}{d\Omega}\right)_0 \frac{1}{\omega}\frac{2\alpha}{\pi}\left[\ln\frac{s}{m_e^2} - 1\right] d\omega. \tag{2.33}$$

Lastly, we must integrate over all energies $d\omega$. However, because of finite detector resolution, the experimental cross section can only be sensitive to those photons radiated over a threshold ΔE, the experimental cross section contains two parts

$$\left(\frac{d\sigma}{d\Omega}\right)_{exp} = \left(\frac{d\sigma}{d\Omega}\right)_{elastic} + \left(\frac{d\sigma}{d\Omega}\right)_{\omega<\Delta E} \tag{2.34}$$

one corresponding to the tree-level cross section, and the other with a radiative correction with $\omega < \Delta E$. When we integrate over $d\omega$, the second term on the right-hand size diverges as can be seen from (2.33).

Thankfully, a brilliant solution to this problem exists. If we assign a mass λ to the radiated photon, the (2.33) becomes

$$\left(\frac{d\sigma}{d\Omega}\right)_{exp} = \left(\frac{d\sigma}{d\Omega}\right)_{elastic} + \left(\frac{d\sigma}{d\Omega}\right)_{\omega<\Delta E} \ln\frac{\Delta E}{\lambda}. \tag{2.35}$$

If we also consider the virtual corrections, such as in Figure 2.8 and calculate the relative cross section, which also contributes to (2.34), we find

$$\frac{d\sigma}{d\Omega} = \left(\frac{d\sigma}{d\Omega}\right)_0 \frac{1}{\omega}\frac{2\alpha}{\pi}\left[\ln\frac{s}{m_e^2} - 1\right] \ln\frac{\lambda}{E} d\omega \tag{2.36}$$

We can sum the real and virtual corrections, and find a total cross section independent from λ! We can now safely take the limit of $\lambda \to 0$ and integrate over ω.

2.5.2 Infrared and Collinear Saftety for Jets

As mentioned in the previous section, infrared and collinear (IRC) divergences will, in theory, exactly cancel. In practice, however, this is not always the case. Depending on the type of jet algorithm used, it may happen that the cancellation breaks and an infinite cross section is calculated. Obviously, this is a problem since the measured cross section will always be finite. It is therefore important from a theoretical standpoint to define in a way that is IRC safe.

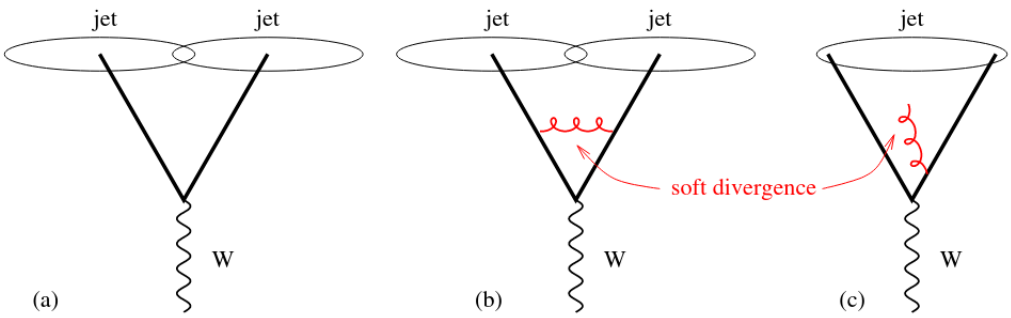

Figure 2.9: A schematic representation of an IR unsafe jet. The emission of a soft gluon changes the event from a two-jet event to a one-jet event due to its effect on the clustering algorithm [14].

An observable $\mathcal{O}$ is said to be IRC safe, respectively, when the following properties are satisfied:

$$\mathcal{O}(X; p_1, \ldots, p_n, p_{n+1}) \to 0) \to \mathcal{O}(X; p_1, \ldots, p_n) \tag{2.37}$$

$$\mathcal{O}(X; p_1, \ldots, p_n \parallel p_{n+1}) \to \mathcal{O}(X; p_1, \ldots, p_n), \tag{2.38}$$

i.e. when the observable reduces to that of n particle case, in absence of the soft or collinear emission. An example of an infrared safe and unsafe jet is shown in Figure 2.9, while Figure 2.10 illustrates an example of a collinear safe and unsafe jet.

The anti-kt algorithm is an example of a jet algorithm which is IRC safe. Due to its weighting, when a soft particle is emitted, this will tend to cluster together with the hard center of the jet. On the other hand, when a particle is emitted collinear to another, the distance Δ_{ij} will be very small, and it will again be clustered together with its parent particle.

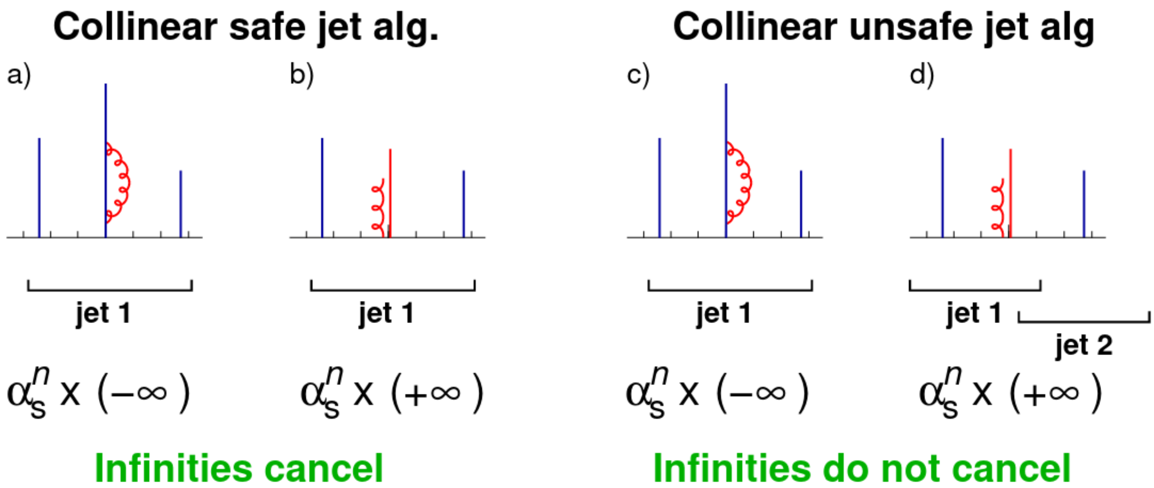

Figure 2.10: A schematic representation of a collinear safe and unsafe jet. The blue lines represent particles, and the length corresponds to the particle's transverse momentum. The horizontal axis represents rapidity. If the emission of a collinear gluon leads to the formation of a second jet, the cancellation is broken and the cross section diverges, as shown on the right. If, on the other hand, it and its parents are treated as a single particle by, for example, summing their momenta, the emission satisfies the definition 2.37 [14].

Chapter 3

Higgs Physics

3.1 Higgs Production Mechanisms

3.2 Higgs Decay Mechanisms

Bibliography

[1] M. Goldhaber, L. Grodzins, and A. W. Sunyar. Helicity of Neutrinos. *Phys. Rev.*, 109:1015–1017, Feb 1958.

[2] Peter W. Higgs. Broken Symmetries and the Masses of Gauge Bosons. *Phys. Rev. Lett.*, 13:508–509, Oct 1964.

[3] Steven Weinberg. A Model of Leptons. *Phys. Rev. Lett.*, 19:1264–1266, Nov 1967.

[4] Gerard 't Hooft. Renormalizable Lagrangians for Massive Yang-Mills Fields. *Nucl. Phys. B*, 35:167–188, 1971.

[5] Mark Thomson. *Modern Particle Physics*. Cambridge University Press, New York, 2013.

[6] L. H. Ryder. *Quantum Field Theory*. Cambridge University Press, 6 1996.

[7] Michael E. Peskin and Daniel V. Schroeder. *An Introduction to Quantum Field Theory*. Addison-Wesley, Reading, USA, 1995.

[8] Antonio Pich. The Standard Model of Electroweak Interactions. In *2010 European School of High Energy Physics*, 1 2012.

[9] Gerry Bunce, Naohito Saito, Jacques Soffer, and Werner Vogelsang. Prospects for spin physics at rhic. *Annual Review of Nuclear and Particle Science*, 50, 08 2000.

[10] Debasish Banerjee, Jajati Nayak, and Raju Venugopalan. Two introductory lectures on high-energy qcd and heavy-ion collisions. *Lecture Notes in Physics*, 785, 10 2008.

[11] Jessica Metcalfe, Simone Seidel, Rouzbeh Allahverdi, Alice Bean, and Igor Gorelov. Development of planar and 3d silicon sensor technologies for the atlas experiment upgrades and measurements of heavy quark production fractions with fully reconstructed d-star mesons with atlas. 08 2021.

[12] George F. Sterman and Steven Weinberg. Jets from Quantum Chromodynamics. *Phys. Rev. Lett.*, 39:1436, 1977.

[13] Matteo Cacciari, Gavin P. Salam, and Gregory Soyez. The anti-k_t jet clustering algorithm. *JHEP*, 04:063, 2008.

[14] Gavin P. Salam. Towards Jetography. *Eur. Phys. J. C*, 67:637–686, 2010.

[15] M. Mangano. QCD and the physics of Hadronic Collisions. *CERN Yellow Rep. School Proc.*, 4:27–62, 2018.